

# Infrared Cavity Ringdown Spectroscopy of Jet-Cooled Polycyclic Aromatic Hydrocarbons

Alex J. Huneycutt,<sup>[a]</sup> Raphael N. Casaes,<sup>[a]</sup> Benjamin J. McCall,<sup>[a, b]</sup> Chao-Yu Chung,<sup>[c]</sup> Yuan-Pern Lee,<sup>[c]</sup> and Richard J. Saykally\*<sup>[a]</sup>

*Infrared absorption spectra of the CH stretching region were observed for naphthalene, anthracene, phenanthrene, pyrene, and perylene using a heated, supersonic, slit-jet source and cavity ringdown spectroscopy. Band positions and intensities recorded with 0.2-cm<sup>-1</sup> resolution were compared with previous gas-phase and argon matrix isolation experiments, as well as theoretical calculations. The largest matrix shift in the absorption maximum (-7.4 cm<sup>-1</sup>) was observed for anthracene, with all others shifted by*

*3.0 cm<sup>-1</sup> or less. Spectral features in the supersonic jet spectrum were generally narrower than those observed in the Ar matrix, with the largest matrix broadening found for the perylene (80% increase). Low number densities observed for the larger polycyclic aromatic hydrocarbons (PAHs) suggest that the lower vapor pressure of PAHs with catacondensed four-membered rings and with five-membered rings other than perylene will not be detectable using our current configuration.*

## Introduction

Polycyclic aromatic hydrocarbons (PAHs), and possibly their substituted derivatives, are important products of incomplete hydrocarbon combustion processes,<sup>[1]</sup> and are now generally acknowledged as an important source of the unidentified infrared bands (UIRs) observed in emission from a variety of environments within the dense interstellar medium.<sup>[2]</sup> The intensity of emission in the six micron C–C stretching region with respect to that in the 3.3–3.4 micron region suggests ionized PAHs as the primary carriers, while the size and structure distribution remains uncertain.<sup>[3]</sup> Efforts to identify carriers among the neutral PAH molecules have largely focused on IR absorption spectra of matrix-isolated species.<sup>[4–7]</sup> These experiments have provided significant insight into the vibrational spectra of this class of molecules, however, matrix spectra are generally subject to spectral shifts and broadening, which can limit their usefulness in comparing with, and interpreting gas-phase spectra.

Acquiring gas-phase direct absorption spectra of PAHs larger than naphthalene have been impeded by their low vapor pressure at reasonable operational temperatures. Samples in static cells heated up to 1000 K have been used to obtain the infrared spectrum of PAHs up to ovalene (10 rings) in size,<sup>[8]</sup> but band broadening in high temperature spectra can prevent the resolution of closely spaced individual vibrational bands in the congested CH stretching region. The heated-cell FTIR spectrum of anthracene,<sup>[9]</sup> recorded at 373 K, will be compared with our gas-phase anthracene spectrum to illustrate the drawbacks of the high temperature experiments, which include enhanced Doppler broadening and the distribution of lower state populations over a much greater number of rotational, and vibrational (hot-band) states.

Low temperature supersonic jet techniques have been combined with visible cavity ringdown spectroscopy to study

the naphthalene cations in direct absorption,<sup>[10]</sup> and with photoinduced cluster dissociation spectroscopy to study Ar or Ne clusters with neutral and cationic phenanthrene, and cationic naphthalene in the 6–20 μm range.<sup>[11, 12]</sup> Room temperature ion trap multiphoton dissociation experiments using a free electron laser have been used to record infrared spectra over the range of 6–20 μm for cations as large as coronene.<sup>[13–15]</sup> However, those techniques are not extendable into the CH stretching region due to the tuning limits of the free electron laser. In addition, modest resolution (> 10 cm<sup>-1</sup>) and room temperature samples would prevent resolution of individual bands in the CH stretching region due to significant band overlap in the spectra.

Optical techniques such as fluorescence spectroscopy, coupled with supersonic jet methods, have been used to obtain the spectrum of perylene<sup>[16–18]</sup> and the spectra of the linear geometry PAHs up to pentacene.<sup>[19]</sup> A novel technique called single photon infrared emission spectroscopy (SPIRES) has been used by our group to obtain the emission spectra of a set of neutral PAHs ranging in size up to coronene<sup>[20–23]</sup> and also the pyrene cation.<sup>[24]</sup> Matrix isolation spectroscopy has also recently been applied to the emission spectra of neutral perylene in a variety of matrices.<sup>[25]</sup>

[a] A. J. Huneycutt, R. N. Casaes, Dr. B. J. McCall, Prof. Dr. R. J. Saykally  
Department of Chemistry, University of California, Berkeley  
Berkeley, CA 94720 (USA)  
Fax: (+1) 510-642-8369  
E-mail: saykally@uclink.berkeley.edu

[b] Dr. B. J. McCall  
Department of Astronomy, University of California, Berkeley  
Berkeley, CA 94720 (USA)

[c] C.-Y. Chung, Prof. Dr. Y.-P. Lee  
Department of Chemistry, National Tsing Hua University  
Hsinchu 30013 (Taiwan)

Here we present the first high-resolution direct absorption spectra of cold, gas-phase, neutral PAHs larger than naphthalene in the CH stretching region. Spectra for both catacondensed (no carbon atom part of more than two rings) and pericondensed (some carbon atoms part of three rings) PAHs were recorded (Figure 1). Since these spectra are recorded for jet-cooled sam-

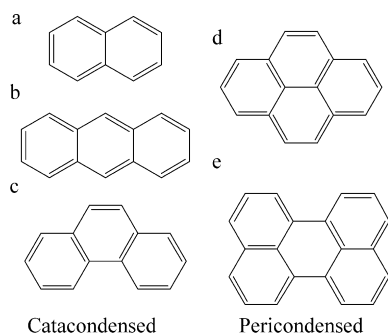


**Figure 1.** Structure of a) naphthalene, b) anthracene, c) phenanthrene, d) pyrene, and e) perylene. If no carbon atoms are part of more than two rings, the structure is referred to as catacondensed. If some carbon atoms are part of three rings, the structure is called pericondensed.

ples,<sup>[26]</sup> rotational temperatures should be similar to temperatures found in the interstellar molecular gas clouds where PAH formation is possible. Low temperatures for internal degrees of freedom result in reduced spectral bandwidths, and offer a significant advantage over heated-cell experiments, wherein thermal effects, including broadening of the neighboring bands in the CH stretching region, can impede assignment of individual transitions and result in thermally induced spectral shifts as large as several wavenumbers at room temperature.<sup>[27]</sup> Also, complications due to matrix-induced perturbations are avoided in the gas-phase spectrum.

## Experimental Section

A heated supersonic slit-jet source, similar to that used for previous studies of the gas-phase spectra of nucleotide bases,<sup>[26]</sup> was used to heat PAH samples up to temperatures of 300 °C. The PAH sample was contained in a compartment below-and open to-the molecular beam source body through which preheated helium carrier gas at a pressure of ~50 psi was passed. The source was operated at 50 Hz with the supersonic jet expanding into a vacuum chamber evacuated by a high throughput Roots pump.

The cavity ringdown spectrometer has been explained in detail elsewhere<sup>[28, 29]</sup> and will be described only briefly. A 50 Hz Nd:YAG (Spectra Physics 290-50, 500 mJ/pulse at 532 nm) pumped dye laser (Lambda Physik FL3002E) was used to generate tunable pulsed visible radiation which was then shifted by three Stokes shifts in a multipass cell containing 14 atm of H<sub>2</sub> gas to produce up to 0.5 mJ/pulse of IR light, tunable out to 10 μm. The dye laser could be operated with an intracavity etalon, which narrowed the laser emission bandwidth from 0.2 cm<sup>-1</sup> to 0.04 cm<sup>-1</sup>. For anthracene, no difference in resolution of spectral features was observed when the system was operated with a laser bandwidth of 0.04 cm<sup>-1</sup>, and all measurements reported here correspond to a laser bandwidth of 0.2 cm<sup>-1</sup>.

The Stokes-shifted radiation was filtered to pass only the desired third-Stokes light, which was subsequently injected into a cavity

formed by two ringdown supermirrors ( $R \approx 0.9998$  at the reflectivity band center). The cavity output was focused onto a liquid N<sub>2</sub>-cooled InSb detector (Infrared Associates,  $D^* \approx 10^{10}$  cm Hz<sup>1/2</sup> W<sup>-1</sup>) and the signal was amplified, digitized, averaged (40 ringdown traces per wavelength point), and fit to a first-order exponential decay. The optical transit time of the cavity divided by the decay constant determined from a single exponential fit of the detector signal gave the per-pass total cavity loss at that wavelength. A typical value for the per-pass loss of the empty cavity at the maximum reflectivity of our 3.3 μm supermirrors was 140 ppm. Spectra were frequency-calibrated with transitions of the  $\nu_3$  band<sup>[30]</sup> of CH<sub>4</sub> to  $\pm 0.1$  cm<sup>-1</sup>.

## Results

It is well known that spectra of species in supersonic jets often exhibit better spectral resolution than flow tube or static cell gas-phase experiments due to significantly reduced Doppler broadening, ultracold rotational temperatures (10 K), and very low vibrational temperatures (< 50 K). These effects help to decongest spectra in regions where band overlap can make assignments difficult or impossible. An example is the heated cell FTIR spectrum of gas-phase anthracene by Cané et al.,<sup>[9]</sup> which shows a profile with features that match the relative intensities and positions of prominent features in the supersonic jet spectrum (although their spectral features are red-shifted by about 5 cm<sup>-1</sup>).

Acquiring the spectrum of anthracene in an argon matrix avoids the problems associated with high temperatures, but adds the additional complication of possible matrix-induced perturbations. Hudgins and Sandford<sup>[5, 6]</sup> have recorded the IR spectra of a large number of PAHs embedded in Ar matrices, and their data will be used here to compare with the supersonic jet spectra. Figure 2 illustrates the differences between the argon matrix isolation spectra (top) reported by Hudgins and Sandford,<sup>[5, 6]</sup> the supersonic jet spectra (bottom) and the band origins<sup>[31]</sup> predicted by Langhoff using density functional theory (stick spectra) for naphthalene, anthracene, phenanthrene, pyrene, and perylene.

Although the Ar matrix spectra were recorded at a lower resolution (0.9 cm<sup>-1</sup>) than the supersonic jet spectra (0.2 cm<sup>-1</sup>), the lower resolution of the matrix experiment does not account for the observed differences. A close inspection reveals several different matrix-induced effects, including spectral shifts and band broadening (Tables 1 and 2). Band positions listed in

**Table 1.** Ar matrix spectral shifts and standard deviation (cm<sup>-1</sup>) with respect to the gas-phase spectrum.

PAH	$\Delta\nu_{\text{avg}}$ <sup>[a]</sup>	$\Delta\nu_{\text{rms}}$	$\sigma$ <sup>[b]</sup>
Naphthalene	0.5	0.5	1.6
Anthracene <sup>[c]</sup>	-2.8	2.6	2.5
Phenanthrene	-1.0	3.0	4.4
Pyrene <sup>[c]</sup>	-0.7	0.7	0.5
Perylene <sup>[c]</sup>	1.2	1.2	2.2

[a] The average of the difference between the band positions in the matrix and gas phase. [b] Standard deviation for the spectral shifts of all peaks within the CH stretching region for each molecule. [c] For the strongest bands only.

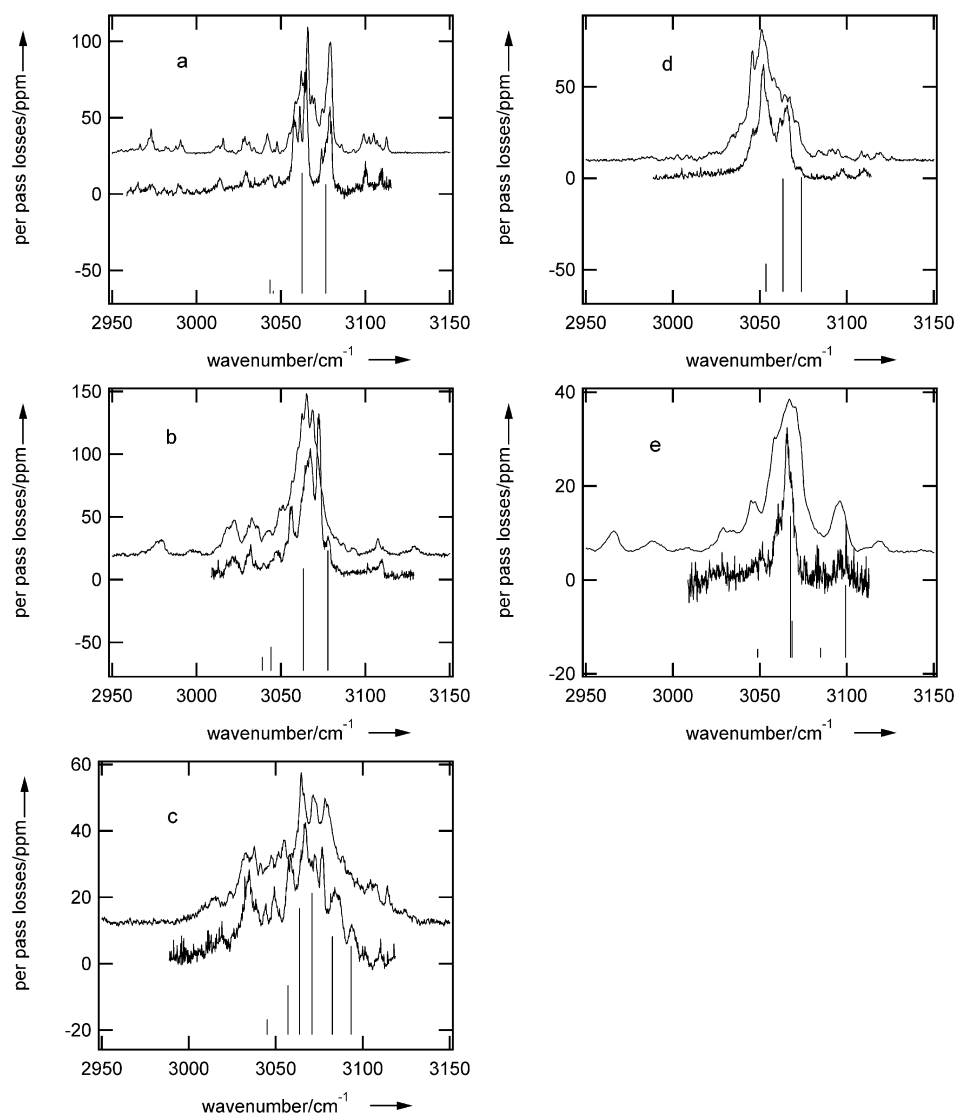


**Figure 2.** Experimental and theoretical IR absorption spectra in the CH stretching region of PAH molecules in the gas-phase and Ar matrix. The spectra are for a) naphthalene, b) anthracene, c) phenanthrene, d) pyrene, and e) perylene. For each graph, the lower trace is the jet-cooled spectrum recorded using cavity ringdown spectroscopy, the upper trace is the 10 K Ar matrix spectrum (from refs. [5, 6]), and the stick spectrum gives the positions and relative intensities of fundamental transitions predicted from density functional theory (from ref. [31]).

**Table 2.** Band half-integrated-area width (HW) and full width at half maximum (FWHM) for PAH spectra ( $\text{cm}^{-1}$ ) in the CH stretching region.

PAH	HW <sup>[a]</sup>			FWHM		
	Gas	Matrix	Ratio <sup>[b]</sup>	Gas	Matrix	Ratio <sup>[b]</sup>
Naphthalene	20	16	0.80	23	21	0.91
Anthracene	15	15	1.0	11	15	1.4
Phenanthrene	31	30	0.97	29	31	1.1
Pyrene	13	14	1.1	18	18	1.0
Perylene	9.5	17	1.8	5.6	19	3.4

[a] HW is defined here as the range centered on the absorption maximum over which one-half of the entire band intensity is bounded. [b] Ratio of matrix value to gas-phase value.

Table 3 to 7 correspond to peaks in the spectra, not necessarily centers of absorption bands. The similarity in band profiles in the Ar matrix and molecular beam spectra, make this a useful way to

compare the two. It should be noted that the values listed here for the Ar matrix spectra differ from those listed in the original publications<sup>[5, 6]</sup> since absorption peaks instead of band centers were used as points of reference. We have also listed the frequencies of many of the weak spectral features that were omitted from the list of band center frequencies in the original publication.<sup>[5, 6]</sup>

The presence of the weak absorption bands in both the supersonic jet and Ar matrix spectra confirm that they are not due to matrix perturbations. Theory does not predict enough fundamental transitions in this region to account for all of the weak features observed.<sup>[31]</sup> Combination bands and overtones of lower frequency CC stretching and CH bending modes are the most likely candidates for assignment. Anthracene, for example, has 66 normal modes, which result in 853 symmetry-allowed binary combination bands. Using the comprehensive list of vibrational frequencies provided by Cané et al.,<sup>[9]</sup> 20 symmetry-allowed binary transitions are within a  $200\text{-cm}^{-1}$  range centered around the CH stretching region. Many modes that would be active through coupling at the binary level do not have IR active fundamentals, in fact, at least one mode is not IR active for all of the binary combinations. If tertiary coupling is considered, the number of trans-

sitions would be much greater. Since experimentally determined frequencies for all the modes of the PAHs used in this study are not available, and given the large number of possible transitions at the binary and tertiary level and the lack of information on the magnitude of anharmonic effects, reliable assignment of all spectral features would be difficult, or impossible, with current data and was not attempted.

Peak positions for the supersonic jet and Ar matrix spectra, as well as theoretical frequencies for vibrational fundamental bands for all PAHs studied here are listed in Tables 3 to 7. Transitions are aligned along each row based on tentative assignments between theoretical frequencies and experimental spectra. Rows without theoretical frequencies are assumed to be overtone or combination band transitions.

Spectral shifts were found to be small in the Ar matrix. From Table 1 it can be seen that the magnitudes of the average of the

**Table 3.** Infrared frequencies ( $\text{cm}^{-1}$ ) in the CH stretching region for naphthalene.

Jet-cooled <sup>[a]</sup>	Ar matrix <sup>[b]</sup> (shift)	Theory <sup>[31]</sup>
2965.3	2966.5 (1.2)	
2973.1	2973 (−0.1)	
2980.9	2981.7 (0.8)	
2989.1	2990.6 (1.5)	
3013.7	3015.7 (2)	
3029.1	3028.7 (−0.4)	
3043.7	3042 (−1.7)	3043.5
3048.9	3047.7 (−1.2)	3045.4
3057.9	3058.4 (0.5)	
3061.1	3062 (0.9)	
3064.1	3065.8 (1.7)	3062.5
3065.1		
3068.5		
3069.9		
3074.1	3074.5 (0.4)	
3079.1	3079.3 (0.2)	3076.5
3098.9		
3102.2		
3100.1	3104.9 (4.8)	
3109.3	3112.6 (3.3)	

[a] This work. [b] Values adapted from data published in ref. [5].

**Table 4.** Infrared frequencies ( $\text{cm}^{-1}$ ) in the CH stretching region for anthracene.

Jet-cooled <sup>[a]</sup>	Ar Matrix <sup>[b]</sup> (shift)	Heated Cell <sup>[9]</sup>	Theory <sup>[31]</sup>
3021.7	3020.7 (−1)		3039.0 <sup>[f]</sup>
3032.1	3032.8 (0.7)	3028	3044.1 <sup>[f]</sup>
3039.5	3042.4 (2.9)		
3047.5	3050.6 (3.1)		
3056.5	3056.4 (−0.1)	3052	
3064.3	3062.5 (−1.8)		
3067.5 <sup>[e]</sup>	3065.1 (−2.4) <sup>[e]</sup>	3061 <sup>[e]</sup>	3063.2 <sup>[e]</sup>
3072.5 <sup>[e]</sup>	3068.5 (−4) <sup>[e]</sup>	3067 <sup>[e]</sup>	3077.8 <sup>[e]</sup>
3077.9			
3109.9	3107.3 (−2.6)		

[a] This work. [b] Values adapted from data published in ref. [5]. [c] Transitions observed or predicted to be the strongest. [d] This assignment is consistent with that of ref. [9], however, it should be considered tentative.

**Table 5.** Infrared frequencies ( $\text{cm}^{-1}$ ) in the CH stretching region for phenanthrene.

Jet-cooled <sup>[a]</sup>	Ar Matrix <sup>[b]</sup> (shift)	Theory <sup>[31]</sup>
3018.7	3014.2 (−4.5)	
3025.3	3023.2 (−2.1)	
3034.7	3032.8 (−1.9)	
3038.5	3037.6 (−0.9)	
3044.3	3041.2 (−3.1)	
3049.1	3047.3 (−1.8)	3045.1
3057.3	3051.6 (−5.7)	
3058.5	3054.7 (−3.8)	3057.0
3066.9	3064.6 (−2.3)	3063.6
3072.3	3071.4 (−0.9)	3070.7
3076.7	3078.1 (1.4)	
3083.9	3088.5 (4.6)	3082.5
3093.7	3104.4 (10.7)	3093.3
3101.3		
3109.7	3114.1 (4.4)	

[a] This work. [b] Values adapted from data published in ref. [5].

**Table 6.** Infrared frequencies ( $\text{cm}^{-1}$ ) in the CH stretching region for pyrene.

Jet-cooled <sup>[a]</sup>	Ar Matrix <sup>[b]</sup> (shift)	Theory <sup>[31]</sup>
3045.9	3045.8 (−0.1)	3053.5
3051.7	3050.9 (−0.8)	3063.2
3058.1		
3061.3	3060.3 (−1)	
3064.5	3064.1 (−0.4)	3073.8
3067.3		
3071.7	3070.4 (−1.3)	
3083.9		
3090		
3094.8		
3108.4		

[a] This work. [b] Values adapted from data published in ref. [5].

**Table 7.** Infrared frequencies ( $\text{cm}^{-1}$ ) in the CH stretching region for perylene.

Jet-cooled <sup>[a]</sup>	Ar Matrix <sup>[b]</sup> (shift)	Theory <sup>[31]</sup>
3022		
3044.9		
3050.3	3047.3 (−3)	3048.7
3060.9	3058.4 (−2.5)	
3065.3	3067 (1.7)	3067.6, 3068.5
3070.4		
	3084.8	
3096.1	3096 (−0.1)	3099.3

[a] This work. [b] Values adapted from data published in ref. [6].

shifts were at most  $3.0 \text{ cm}^{-1}$ , with some of the PAHs experiencing a red-shift (anthracene, phenanthrene, and pyrene) and others a blue-shift (naphthalene and perylene). The standard deviations of the spectral shifts across the CH stretching region were larger—up to  $4.4 \text{ cm}^{-1}$  for phenanthrene.

The largest shift in the absorption maximum across the entire band was observed for anthracene (Figure 3). A spectral shift and difference in relative intensities of the individual transitions between the jet-cooled and Ar matrix spectra result in an apparent matrix-induced red-shift in the absorption maximum of  $7.4 \text{ cm}^{-1}$ . Given the high resolution and low temperature of the

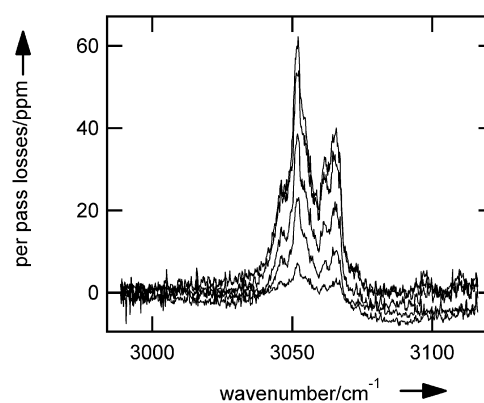


**Figure 3.** Gas-phase spectra of pyrene for source temperatures of (weakest to strongest) 445, 472, 491, 504, and 520 K. The band intensity was observed to increase with increasing temperature without distortions such as broadening of the bands or the appearance of additional peaks.

jet-cooled spectrum, the band shifts of the individual transitions could be determined and the matrix red-shift was found to be  $2.8\text{ cm}^{-1}$  for the three strongest transitions.

Phenanthrene had the greatest number of fundamental transitions predicted (6) in the CH stretching region. In the observed Ar matrix spectrum, the CH stretching modes occurred over a larger range than in the jet-cooled spectrum. The increase in range was only  $8.9\text{ cm}^{-1}$ , or about a 10% increase from the range in the gas-phase spectrum, but resulted in the largest observed standard deviation for the spectral shifts across the CH stretching band ( $\sigma = 4.4\text{ cm}^{-1}$ ). All of the spectral features correlated well between the two matrix and gas-phase spectra, although small differences in intensity and distance between peaks did occur as can be seen in Figure 2c.

In addition to the spectral shifts, Ar matrix features were generally broader. Broadening of the entire band refers to an increase in "width", where width is here defined as the range centered around the largest peak in which one-half of the integrated area of the band is bounded. We will introduce the term half-integrated-area width and use the acronym HW to refer to this measurement. While this is at best a crude measure of comparison between complex absorption bands, it helps to elucidate general matrix broadening effects for this class of molecules. We have reported the HW and the full width at half maximum (FWHM) associated with the gas-phase and Ar matrix spectra of each PAH in Table 2.

Perylene exhibited the largest degree of matrix-induced broadening that was observed for any of the PAHs, as can be seen in Figure 2e. Although the spectral shift of the absorption maxima between the jet-cooled and Ar matrix spectra was only  $1.7\text{ cm}^{-1}$ , the Ar matrix perturbed the system sufficiently to produce an increase in the HW by a factor of 1.8, and an increase in FWHM by a factor of 3.4.

Low number densities for perylene gave rise to reduced absorption band strength (see Figure 2e). With a molecular structure of six conjoined rings (see Figure 1e), perylene was the largest PAH studied. Even at the highest operational temperature for stable performance of the supersonic jet source (572 K), a number density of only  $1.7 \times 10^{12}\text{ cm}^{-3}$  was observed and calculated using the integrated absorption strength and the theoretical band strength from density functional theory.<sup>[31]</sup> Catacondensed four-ring and five-ring PAHs other than perylene should have vapor pressures low enough that number densities would be below the detection limit of our spectrometer.

## Implications for Analysis of Ar Matrix Spectra

The goal of this work was to calibrate the effects that Ar matrices had on the spectra of PAHs in the CH stretching region. From the comparison of gas-phase to matrix spectra, it is apparent that the spectral shifts in the CH stretching region are small, although they appear slightly larger than the shifts of the lower frequency CC stretching and CH bending modes in the case of anthracene.<sup>[9]</sup> The average spectral shift in the argon matrix for anthracene, phenanthrene, and pyrene were small red-shifts with respect to the gas-phase spectra, whereas small blue-shifts were observed for naphthalene and perylene, but all were less

than about  $3\text{ cm}^{-1}$  in magnitude. However, as illustrated in the anthracene spectrum, a combination of spectral shifts and differences in relative intensity between peaks can cause a change in the absorption maximum across the entire band that is significantly larger than the spectral shifts of individual peaks. This effect can be significant when comparing matrix spectra to gas-phase spectra taken with lower instrument resolution, or with higher sample temperature.

Spectral broadening and variation in relative intensity between bands was much more inconsistent than was the magnitude of the spectral shifts. The HW of the Ar matrix spectra varied from 20% smaller for naphthalene to 80% larger for perylene. The HW of the anthracene spectrum increased in the matrix by 9%, and for pyrene by 10%, while the HW decreased for phenanthrene by 3%. Since the decrease in HW observed for naphthalene resulted from intensity increase between the two main spectral features and not a true decrease in HW of the individual bands, the general trend appears to be a broadening of spectral features in the matrix. The exact degree of matrix broadening was difficult to quantify. Differences in FWHM between the matrix and gas-phase spectra were similar to the HW measurements, although both quantities are imperfect measurements of matrix effects for such complex band shapes.

Many weak transitions were observed in the CH stretching region with relative intensities and frequencies that correlate well with features in the Ar matrix spectra. The number of vibrational modes for molecules as large as PAHs give rise to large numbers of binary and tertiary combination bands, which are likely to account for the many weak transitions observed in the CH stretching region.

The preceding analysis suggests that CH stretching transition frequencies determined for PAHs from Ar matrix spectra should be accurate to within  $< 5\text{ cm}^{-1}$  and should exhibit very similar band shapes, although slightly broadened, compared to the rotationally cold gas-phase spectra.

## Conclusions

The direct absorption spectra in the CH stretching region of rotationally cold gas-phase naphthalene, anthracene, phenanthrene, pyrene, and perylene have been reported for the first time. A detailed analysis indicates that similarity of the Ar matrix spectra to the gas-phase spectra is sufficient in this region to compare the band shapes and positions with reasonable accuracy. Previously reported density functional theoretical predictions of the band origins were found to be very reliable for the fundamental transitions in the gas-phase spectra of all the PAHs studied.

Spectral features that were not attributable to fundamental transitions are most likely due to overtones and combination bands of lower frequency modes such as C–C stretching and C–H bending modes. Considering only symmetry allowed binary combinations, 20 combination bands were predicted to occur for anthracene within a  $200\text{ cm}^{-1}$  range about the C–H stretching region.

Comparing the supersonic jet and Ar matrix spectra indicated two matrix-induced effects—broadening of absorption bands, and a shift of the absorption peaks. Absorption bands were generally broader in the argon matrix spectra, but the irregularity of the bands made the magnitude of the difference difficult to quantify. Spectral shifts of  $\Delta\nu_{\text{rms}} \leq 3.0 \text{ cm}^{-1}$  were observed for the spectra of all PAHs studied, however, the shift was that of an average red-shift for anthracene, phenanthrene, and pyrene, and that of an average blue-shift for naphthalene and perylene. The close similarity between the gas phase and Ar matrix spectra for the PAHs investigated here suggest that the matrix perturbations for this class of molecules result in spectral shifts of only several wavenumbers, and moderate broadening of spectral features.

### Acknowledgements

The authors would like to thank D. Hudgins for providing the Ar matrix absorption data previously published in ref. [5, 6]. This work was supported by the Chemical Dynamics Program of the AFOSR and by the Laboratory Astrophysics Program of NASA. B.J.M. is supported by the Miller Institute for Basic Research in Science.

**Keywords:** cavity ringdown spectroscopy · IR spectroscopy · matrix isolation · polycyclic aromatic hydrocarbons

- [1] M. Frenklach, *Phys. Chem. Chem. Phys.* **2002**, *4*, 2028.
- [2] F. Salama, in *Solid Interstellar Matter: The ISO Revolution* (Eds.: L. d'Hendecourt, C. Joblin, A. Jones), Springer-Verlag, New York, **1999**, 65.
- [3] L. J. Allamandola, D. M. Hudgins, S. A. Sandford, *Astrophys. J.* **1999**, *511*, L115.
- [4] M. Vala, J. Szczepanski, F. Pauzat, O. Parisel, D. Talbi, Y. Ellinger, *J. Phys. Chem.* **1994**, *98*, 9187.
- [5] D. M. Hudgins, S. A. Sandford, *J. Phys. Chem. A* **1998**, *102*, 329.
- [6] D. M. Hudgins, S. A. Sandford, *J. Phys. Chem. A* **1998**, *102*, 344.
- [7] C. W. J. Bauschlicher, S. R. Langhoff, S. A. Sandford, D. M. Hudgins, *J. Phys. Chem. A* **1997**, *101*, 2414.
- [8] C. Joblin, L. d'Hendecourt, A. Léger, D. Défourneau, *Astron. Astrophys.* **1994**, *281*, 923.
- [9] E. Cané, A. Miani, P. Palmieri, R. Tarroni, A. Trombetti, *J. Chem. Phys.* **1997**, *106*, 9004.
- [10] D. Romanini, L. Biennier, F. Salama, A. Kachanov, L. J. Allamandola, F. Stoeckel, *Chem. Phys. Lett.* **1999**, *303*, 165.
- [11] H. Piest, J. Oomens, J. Bakker, G. von Helden, G. Meijer, *Spectrochim. Acta, Part A* **2001**, *57*, 717.
- [12] J. A. Piest, G. von Helden, G. Meijer, *Astrophys. J.* **1999**, *520*, L75.
- [13] J. Oomens, A. J. A. van Rooij, G. Meijer, G. von Helden, *Astrophys. J.* **2000**, *542*, 404.
- [14] J. Oomens, B. G. Sartakov, A. G. G. M. Tielens, G. Meijer, G. von Helden, *Astrophys. J.* **2001**, *560*, L99.
- [15] J. Oomens, G. Meijer, G. von Helden, *J. Phys. Chem. A* **2001**, *105*, 8302.
- [16] S. A. Schwartz, M. R. Topp, *Chem. Phys.* **1984**, *86*, 245.
- [17] B. Fourmann, C. Jouvét, A. Tramer, J. M. le Bars, P. Millie, *Chem. Phys.* **1985**, *92*, 25.
- [18] C. Bouzou, C. Jouvét, J. B. Le Blond, P. Millie, A. Tramer, M. Sulkes, *Chem. Phys. Lett.* **1983**, *97*, 161.
- [19] A. Amirav, U. Even, J. Jorner, *Chem. Phys. Lett.* **1980**, *72*, 21.
- [20] S. Schlemmer, D. J. Cook, J. A. Harrison, B. Wurfel, W. Chapman, R. J. Saykally, *Science* **1994**, *265*, 1686.
- [21] D. R. Wagner, H.-S. Kim, R. J. Saykally, *Astrophys. J.* **2000**, *545*, 854.
- [22] D. J. Cook, S. Schlemmer, N. Balucani, D. R. Wagner, J. A. Harrison, B. Steiner, R. J. Saykally, *J. Phys. Chem. A* **1998**, *102*, 1465.
- [23] D. J. Cook, S. Schlemmer, N. Balucani, D. R. Wagner, B. Steiner, R. J. Saykally, *Nature* **1996**, *380*, 227.
- [24] H.-S. Kim, D. R. Wagner, R. J. Saykally, *Phys. Rev. Lett.* **2001**, *86*, 5691.
- [25] C. Joblin, F. Salama, L. Allamandola, *J. Chem. Phys.* **1999**, *110*, 7287.
- [26] K. Liu, R. S. Fellers, M. R. Viant, R. P. McLaughlin, M. G. Brown, R. J. Saykally, *Rev. Sci. Instrum.* **1996**, *67*, 410.
- [27] C. Joblin, P. Boissel, A. Léger, L. d'Hendecourt, D. Défourneau, *Astron. Astrophys.* **1995**, *299*, 835.
- [28] A. J. Huneycutt, R. J. Stickland, F. Hellberg, R. J. Saykally, *J. Chem. Phys.* **2003**, *118*, 1221.
- [29] J. B. Paul, R. A. Provencal, R. J. Saykally, *J. Phys. Chem. A* **1998**, *102*, 3279.
- [30] A. H. Nielsen, H. H. Nielsen, *Phys. Rev.* **1935**, *48*, 864.
- [31] S. R. Langhoff, *J. Phys. Chem.* **1996**, *100*, 2819.

Received: April 7, 2003 [F 776]

Revised: December 15, 2003